Analyst

Cite this: *Analyst*, 2012, **137**, 2799

www.rsc.org/analyst

PAPER

Amplified fluorescence detection of mercury(II) ions (Hg^{2+}) using target-induced DNAzyme cascade with catalytic and molecular beacons

Lin Qi,[a] Yongxi Zhao,*[a] Hui Yuan,[b] Kai Bai,[b] Yue Zhao,[a] Feng Chen,[a] Yanhua Dong[a] and Yayan Wu[a]

Received 1st April 2012, Accepted 16th April 2012
DOI: 10.1039/c2an35437c

In this work, a fluorescent sensing strategy was developed for the detection of mercury(II) ions (Hg^{2+}) in aqueous solution with excellent sensitivity and selectivity using a target-induced DNAzyme cascade with catalytic and molecular beacons (CAMB). In order to construct the biosensor, a Mg^{2+}-dependent DNAzyme was elaborately designed and artificially split into two separate oligonucleotide fragments. In the presence of Hg^{2+}, the specific thymine–Hg^{2+}–thymine (T–Hg^{2+}–T) interaction induced the two fragments to produce the activated Mg^{2+}-dependent DNAzyme, which would hybridize with a hairpin-structured MB substrate to form the CAMB system. Eventually, each target-induced activated DNAzyme could catalyze the cleavage of many MB substrates through true enzymatic multiple turnovers. This would significantly enhance the sensitivity of the Hg^{2+} sensing system and push the detection limit down to 0.2 nM within a 20 min assay time, much lower than those of most previously reported fluorescence assays. Owning to the strong coordination of Hg^{2+} to the T–T mismatched pairs, this proposed sensing system exhibited excellent selectivity for Hg^{2+} detection, even in the presence of 100 times of other interferential metal ions. Furthermore, the applicability of the biosensor for Hg^{2+} detection in river water samples was demonstrated with satisfactory results. These advantages endow the sensing strategy with a great potential for the simple, rapid, sensitive, and specific detection of Hg^{2+} from a wide range of real samples.

Introduction

Water-soluble mercury(II) ions (Hg^{2+}), the most usual and stable inorganic form of mercury pollution, are highly toxic to human health and the environment, even at low concentration. The accumulation of Hg^{2+} in vital organs will cause long-term adverse effects on biological systems including DNA damage, inhibition of ligand–receptor interactions, and the disruption of the immune system at the cellular level, which results in a number of severe health problems such as brain damage, kidney failure, and various cognitive and motion disorders.[1,2] Thus, the detection of Hg^{2+} is of extreme importance to deal with these environmental and health problems. So far, several analytical techniques, including cold-vapor atomic fluorescence spectrometry (CV-AFS),[3] cold-vapor atomic absorption spectroscopy (CV-AAS),[4] inductively coupled plasma atomic emission spectrometry (ICP-AES),[5] and inductively coupled plasma mass spectrometry (ICP-MS),[6] have been extensively applied in the detection of Hg^{2+}. Although these methods meet the standard of the US Environmental Protection Agency (EPA) for the maximum allowable level (MAL) of Hg^{2+} in drinking water (10 nM, 2 ppb), the requirements of trained professional operators, complicated and expensive instrumentation, or time-consuming sample preparation processes make them unsuitable for facile on-site and real-time detection of Hg^{2+} in real samples.

The recent discovery of Hg^{2+}-mediated thymine–thymine (T–T) DNA base-pairing by Ono and co-workers has prompted the development of novel approaches for overcoming the above-mentioned drawbacks.[7,8] The binding constant of this T–Hg^{2+}–T base pair in DNA duplexes is higher than that of a T–A Watson–Crick pair.[9] By utilizing the strong T–Hg^{2+}–T interaction, numerous Hg^{2+} detection methods including fluorescent,[7,10–18] colorimetric,[19–21] and electrochemical biosensors[22,23] have been developed. Thanks to the high specificity of T–Hg^{2+}–T coordination chemistry, these sensing strategies exhibit excellent selectivity for Hg^{2+} detection against the interferences of other metal ions. Nevertheless, most of them are limited in their practical use due to their insufficient sensitivity. More recently, many novel sensing systems have been proposed for improving the sensitivity of Hg^{2+} detection based on isothermal nucleic acid amplification,[24–26] nanotechnology,[27,28] chemiluminescence,[29,30] and other detection techniques.[31–33] However, these methods either suffer from requiring multi-step processes or involve high-cost equipment, and complicated synthesis of probe materials.

[a]*Key Laboratory of Biomedical Information Engineering of Education Ministry, School of Life Science and Technology, Xi'an Jiaotong University, Xi'an, Shaanxi 710049, P. R. China. E-mail: yxzhao@mail.xjtu.edu.cn*
[b]*Shaanxi Tobacco Quality Supervision and Test Station, Shaanxi Branch of China National Tobacco Corporation, Xi'an, Shaanxi 710061, P. R. China*

Therefore, the development of novel approaches for the simple, rapid, cost-effective, highly sensitive and selective determination of Hg^{2+} is still an urgent demand.

As a new potential biocatalyst for signal generation and amplification, DNAzymes (also called deoxyribozymes or catalytic DNAs) have attracted particular attention in the development of various sensing systems during the past decade.[34–36] DNAzymes are single stranded nucleic acids with a particular sequence which are isolated from combinatorial oligonucleotide libraries by *in vitro* selection[37] and possess high catalytic activities toward specific substrates.[38] Similar to protein enzymes or ribozymes, DNAzymes can also catalyze many biochemical reactions, and some of the reactions require specific metal ions as cofactors.[34] More importantly, DNAzymes offer several advantages over these conventional enzymes, such as easier synthesis, having a higher stability to resist hydrolysis and retaining their activities after repeated denaturation and renaturation, and relatively lower production costs.[39] All these unique features make DNAzymes an excellent and versatile platform for sensing Hg^{2+}, even in real samples. Hollenstein *et al.* reported a new, self-cleaving DNAzyme (10–13 DNAzyme) with high specificity toward Hg^{2+}.[40] Nevertheless, the sensing system-based DNAzyme showed a slightly higher detection limit of 100 nM (20 ppb) due to its lower catalytic efficiency. Utilizing the Hg^{2+}-mediated T–T base pair to modulate the proper folding of G-quadruplex DNAs and inhibit the DNAzyme activity, Wang's group constructed a label-free colorimetric sensor, which enabled aqueous Hg^{2+} to be detected at 50 nM (10 ppb) with high selectivity in a facile way.[21] In order to improve the sensitivity, the T–Hg^{2+}–T interaction was further used to engineer an allosteric UO_2^{2+}-dependent DNAzyme for selective Hg^{2+} detection with a detection limit down to 2.4 nM (0.48 ppb).[16] However, the labelling on the 3′-end and extact composition in the catalytic core more or less had a negative effect on the performance of the DNAzyme, and uranium might cause health and environmental problems due to its radioactivity. To overcome these limitations, a label-free and environmental-friendly Mg^{2+}-dependent DNAzyme has been exploited for Hg^{2+} sensing.[41] In this strategy, the Hg^{2+}-mediated T–T base pair in the variable stem region nearly had no effect on the catalytic efficiency of the DNAzyme which resulted in a lower detection limit of l.0 nM (0.2 ppb). Nevertheless, the low quenching efficiency of the catalytic beacon caused a high fluorescence background, making it difficult to take advantage of the true potential of the catalytic beacon in signal amplification through multiple enzymatic turnovers.[42] More seriously, a sensing procedure needing 180 min was extremely time-consuming, which limited its utility in routine monitoring.

More recently, a so-called catalytic and molecular beacons (CAMB) strategy has emerged as a versatile platform for various sensor syetems.[43–45] In comparison with the original catalytic beacon, the new CAMB strategy possesses unique features, such as the dramatically low background fluorescence, and high stability without any interference from the ratio of DNAzyme to MB substrate, which makes it possible to use excess CAMB for a higher fluorescent signal through cycling and regenerating the DNAzyme. Inspired by these researches, we developed a highly sensitive and selective fluorescent biosensor for the detection of Hg^{2+} in aqueous solution using the T–Hg^{2+}–T coordination-induced DNAzyme cascade with the CAMB strategy. This proposed strategy combined low-background CAMB substrates and the true enzymatic multiple turnover (one DNAzyme involves in the cleavage of a number of substrates), which significantly improved the sensitivity of the biosensor with the detection limit down to 0.2 nM within a 20 min assay time. Moreover, the strong T–Hg^{2+}–T binding ensured that the sensing system could specifically distinguish the target Hg^{2+} from other competing metal ions. The proposed sensing system was further applied to the detection of Hg^{2+} in river water samples with satisfactory results.

Experimental

Materials and chemicals

Metal salts ($Hg(NO_3)_2$, $Pb(NO_3)_2$, $Cd(NO_3)_2$, NaCl, KCl, $MgCl_2$, $CaCl_2$, $AlCl_3$, $FeCl_2$, $FeCl_3$, $ZnCl_2$, $CrCl_3$, $CoCl_2$, and $SnCl_2$) and HEPES (4-(2-hydroxyethyl)-1-piperazineethanesulfonic acid) were purchased from Sigma-Aldrich (St. Louis, MO). A stock solution of Hg^{2+} was prepared by dissolving $Hg(NO_3)_2$ with 0.5% HNO_3. All other solutions were prepared and diluted by DEPC-treated Milli-Q water (resistance > 18.2 MΩ) directly without any further purification. Oligonucleotides used in this study were synthesized and HPLC purified by Shanghai Sangon Biotechnology Co., Ltd (Shanghai, China). Their sequences were:

Probe 1

5′-**TT**CG**TT**GAC**TT**CACACCCATGTACCAAGCAT-3′

Probe 2

5′-ATACCGACAGCGATTG**TT**GTC**TT**CGTA-3′

MB substrate

5′-FAM-CACCACTACAAATTATGCTTGGT-TrAGGTCGGTATACGAGCGTGTGGTG-DABCYL-3′

The underlined and bold letters in Probe 1 and Probe 2 represent the catalytic core and five T–T mismatched bases in the stem–loop region of the Mg^{2+}-dependent DNAzyme, respectively.

Apparatus

Fluorescence measurements were performed using a FluoroMax-4 fluorescence spectrometer (Horiba Jobin Yvon) at room temperature. The emission spectra were collected from 505 nm to 540 nm with an excitation wavelength of 495 nm. The fluorescence intensity at 518 nm was used to choose the optimal experimental conditions and evaluate the performance of the proposed sensing system. Both the excitation and emission slit widths were set at 3 nm.

Optimization of sensing conditions

To investigate the effect of experimental conditions on the performance of the Hg^{2+} sensing system, a fixed concentration of Probe 1 (20 nM), Probe 2 (20 nM), NaCl (1 M), and Mg^{2+} (10 mM) were mixed in HEPES buffer (250 mM HEPES) with 20 nM Hg^{2+} by varying the molar ratio of DNAzyme to MB substrate (1/1, 1/2, 1/3, 1/4, 1/5 and 1/6), the buffer pH (5.5, 6.0, 6.5, 7.0, 7.5 and 8.0), and the incubation temperature (15 °C, 20 °C, 25 °C, 30 °C, 35 °C and 40 °C). The reaction was allowed to proceed for 30 min prior to fluorescence measurement.

Subsequently, a time interval set at 5 min was used to monitor the time-dependent fluorescence response in order to choose the optimal time for the Hg^{2+} sensing system.

Amplified fluorescence detection of Hg^{2+}

The detection was carried out in a HEPES buffer (250 mM HEPES, 1 M NaCl, 10 mM Mg^{2+}, pH = 7.0) containing Probe 1 (20 nM), Probe 2 (20 nM), and the MB substrate (80 nM). For the sensitivity evaluation, different concentrations of Hg^{2+} (0–320 nM) were added into the system, and the solutions were incubated at 30 °C for 20 min prior to the fluorescence measurement. For the selectivity evaluation, the fluorescence response of 20 nM Hg^{2+} was compared with 13 types of interferential metal ions (K^+, Na^+, Ca^{2+}, Mg^{2+}, Al^{3+}, Zn^{2+}, Fe^{2+}, Fe^{3+}, Pb^{2+}, Cd^{2+}, Sn^{2+}, Co^{2+} and Cr^{3+}, 2 μM) and the mixture of them (1.3 μM).

Real sample analysis

River water samples were collected from Xi'an Chan River and were filtered through a 0.2 μM membrane. For the recovery test, aliquots of the river water samples were spiked with standard solutions of Hg^{2+} over the concentrations from 0.0 to 1.0 μM. Subsequently, the spiked water samples were mixed with Probe 1 (20 nM), Probe 2 (20 nM), and the MB substrate (80 nM) in HEPES buffer and incubated at 30 °C for 20 min prior to fluorescence measurement.

Results and discussion

Sensing strategy

The designed strategy is conceptually depicted in Scheme 1. The Mg^{2+}-dependent DNAzyme was selected as the biocatalyst for signal amplification based on its highly catalytic activity and the ability to change the stem sequences of the hairpin structure for expanding its functionality without losing DNAzyme activity.[42] Except for the highly conserved 15 nucleotides in the catalytic core, there were two arm regions with 6–12 nucleotides at each end of the DNAzyme strand which could bind to the complementary substrate *via* Watson–Crick base-pairing.[42] It was demonstrated that the longer arm sequences could facilitate the hybridization of the DNAzyme with the substrate and enhance the enzyme-catalyzed hydrolysis reaction of the substrate. However, if the arm length is too long, it will also reduce the releasing kinetics of the cleaved products from the DNAzyme, leading to a poor sensing performance.[45] Another concern is that more complementary base pairs between the arm sequences and the loop sequence of the MB substrate would result in a higher background signal in the absence of Hg^{2+}. To overcome the limitations, the DNAzyme was artificially split into two separate oligonucleotide fragments, Probe 1 and 2, which included the changeable stem sequences (domain I, marked in blue), the highly conserved sequences of catalytic core (domain II, marked in deep red), and the arm sequences (domain III, marked in green), respectively. And the domain III sequences were designed with 8 and 9 bases perfectly complementary to each side of the cleavage site in the loop region of the MB structured substrate, respectively. The melting temperature (T_m) values of the two duplexes were calculated to be no more than 26 °C, which prevented the formation of stable hybridization between the separate DNAzyme and MB substrate under the reaction temperature of 30 °C. The domain I sequences were elaborately designed to contain eight complementary base pairs separated by five T–T mismatches for avoiding the formation of the active secondary structure in the catalytic core. In the presence of Hg^{2+}, the domain I would bind to each other through strong T–Hg^{2+}–T interaction and complementary base-pairing, enabling the two separate fragments of the DNAzyme to form a stem–loop structure, thereby restoring its catalytic activity. Subsequently, the activated DNAzyme hybridized with a hairpin-structured MB substrate through the complementary arm sequences and catalyzed the cleavage of the MB substrate in the presence of cofactor Mg^{2+}. After cleavage, the activated DNAzyme dissociated from the cleaved MB substrate, and the quenched MB fluorophore/quencher pair separated from each other, resulting in fluorescence signal enhancement. The released DNAzyme could then hybridize with another MB substrate and be re-used for the second cycle of cleavage. Eventually, each target-induced activated DNAzyme can go through many cycles to realize the cleavage of many MB substrates, achieving the amplified fluorescence signal for target Hg^{2+}. By contrast, in the absence of target Hg^{2+}, Probe 1 and 2 alone could not form a stable stem–loop and active structure, and hybridize with the hairpin-structured MB substrate to catalyze the cleavage of the substrate, due to five T–T mismatches and short complementary arm sequences. Therefore, there was no fluorescence enhancement. In this way, we successfully converted each Hg^{2+}-induced DNAzyme activation event into the detectable fluorescent signals, which were significantly amplified by cycling and regenerating the activated DNAzyme to realize the cleavage of many MB substrates in a one-step detection fashion.

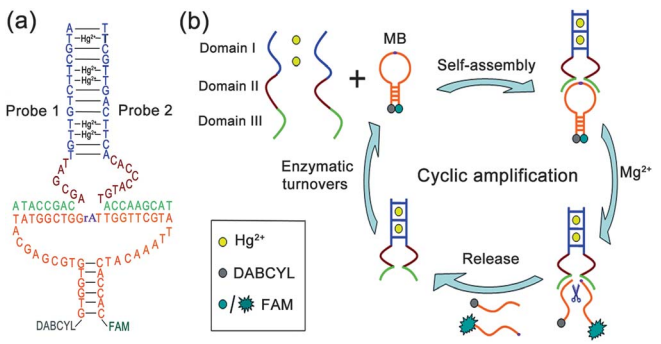

Scheme 1 (a) Secondary structure of the T–Hg^{2+}–T coordination-induced activated DNAzyme on CAMB, (b) schematic of target-induced DNAzyme cascade with CAMB for the amplified fluorescence detection of Hg^{2+}.

Typical fluorescence responses of the sensing system toward target Hg^{2+} are shown in Fig. 1. It could be observed that the addition of probes only caused a negligible enhancement of the background fluorescence of the MB substrates. However, compared with the background fluorescence in the presence of Probe 1 and 2, the amplification strategy would result in an approximate 7.5-fold fluorescence enhancement upon the

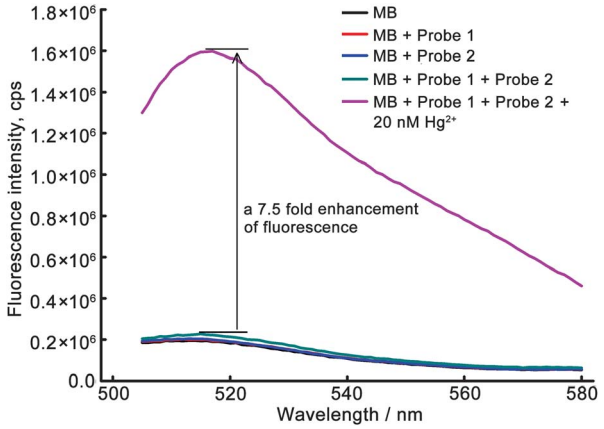

Fig. 1 Fluorescence responses of the proposed sensing system toward Hg^{2+} under different conditions in the presence of 10 mM Mg^{2+}.

addition of 20 nM Hg^{2+}. The results provided a convincing proof of the detection mechanism and design feasibility of the amplified sensing system.

Optimization of the experimental conditions

In order to achieve the sensing system's best performance, several important conditions were subsequently optimized at a fixed concentration of Hg^{2+} of 20 nM as shown in Fig. 2. Owing to the fact that each target-induced activated DNAzyme could undergo many cycles to cleave a number of MB substrates for obtaining the amplified fluorescent signal, there must be an excess of MB substrates involved in our sensing system, and an appropriate molar ratio of the DNAzyme to MB substrate will be a key factor that significantly affects the sensing performance. Therefore, the effect of molar ratio was investigated with a fixed concentration of DNAzyme of 20 nM and various concentrations of MB substrates from 20 nM to 160 nM, which is shown in Fig. 2a. The fluorescence response increased with the increasing concentration of MB substrates. And the ratio of maximum fluorescence enhancement (F/F_0) was observed when the ratio of the DNAzyme to MB substrate reached 1 : 4, which confirmed the capability of each target-induced activated DNAzyme to catalyze the cleavage of several MB substrates. Although the Hg^{2+}-induced fluorescence response still followed an increasing trend with further increase in MB concentration, the F/F_0 exhibited a gradual decrease due to a much higher background fluorescence caused by the greater excess of MB substrates. Therefore, the molar ratio of 1 : 4 was used for the subsequent investigation.

It has been reported that the fluorescence intensity of the FAM fluorophore linked to the MB substrate can be significantly enhanced with the increase of pH.[45] The effect of buffer pH on the sensing performance was investigated over a pH range from 5.5 to 8.0 and the results are depicted in Fig. 2b. As can be seen, both the fluorescence response and background fluorescence intensity increased with the increase of buffer pH. However, as the buffer pH increased continuously, the fluorescence decreased gradually. This might be due to the instability of Hg^{2+} in an alkaline environment when the buffer pH went beyond 7.0. Thus, pH 7.0 was chosen as the optimal pH of the reaction buffer for further experiments as F/F_0 was maximised here.

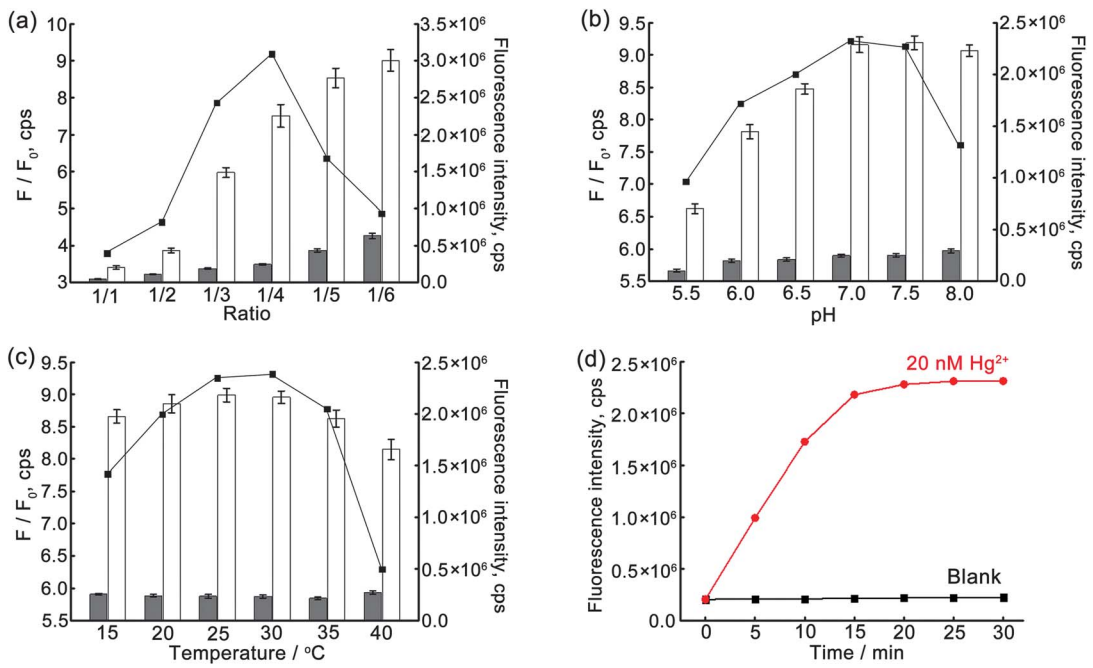

Fig. 2 Optimization of the experimental conditions. The influence of (a) the ratio of Mg^{2+}-dependent DNAzyme to MB substrate, (b) the buffer pH, (c) the reaction temperature on the fluorescence response of the sensing system, (d) the time-dependent fluorescence response over background fluorescence with 20 nM Hg^{2+}. The gray and white bars represent the fluorescence intensity at 518 nm of this sensing system in the absence (F) and presence (F_0) of 20 nM Hg^{2+}, respectively. The lines represent the fluorescence enhancement (F/F_0). The error bars denote the standard deviations for measurements taken from three independent experiments.

Since the reaction temperature could affect the thermal stability of the DNAzyme–substrate duplex and the MB substrate, different reaction temperatures were also investigated, and the dependence of the fluorescence signals on the reaction temperature is shown in Fig. 2c. When the reaction temperature was 25 °C, the maximum fluorescence response was achieved. By contrast, the minimum background fluorescence intensity was observed while the reaction temperature reached 30 °C. Thereafter, the background fluorescence intensity exhibited a gradual decrease with a further decrease in reaction temperature. This was probably because the lower reaction temperature facilitated the formation of the two separate DNAzyme–MB substrate duplexes, resulting in the instability of the MB substrates with an enhanced background fluorescent signal. Although the higher reaction temperature could avoid the problem, it would destroy the stability of the hairpin-structured MB substrate, leading to higher background fluorescence. Finally, the maximum F/F_0 was obtained at the reaction temperature of 30 °C. Therefore, 30 °C was selected for the further investigation. Furthermore, the concentration of cofactor Mg^{2+} was examined over a range from 0 to 40 mM. It was found that F/F_0 increased remarkably with the increase of the Mg^{2+} concentration, and then leveled off when the Mg^{2+} concentration exceeded 10 mM. Finally, 10 mM Mg^{2+} was selected for our sensing system (data not shown).

All the above-mentioned optimizations were carried out at a constant reaction time of 30 min. For achieving the faster sensing response, we further investigated the time-dependent fluorescence response over background fluorescence with 20 nM Hg^{2+}. The results are shown in Fig. 2d. As can be seen, the fluorescence response was quickly enhanced with the increase in reaction time, and nearly reached a plateau after 20 min, while the background fluorescence intensity remained almost unchanged. Thus, 20 min was selected as the optimal reaction time of our sensing system in all experiments.

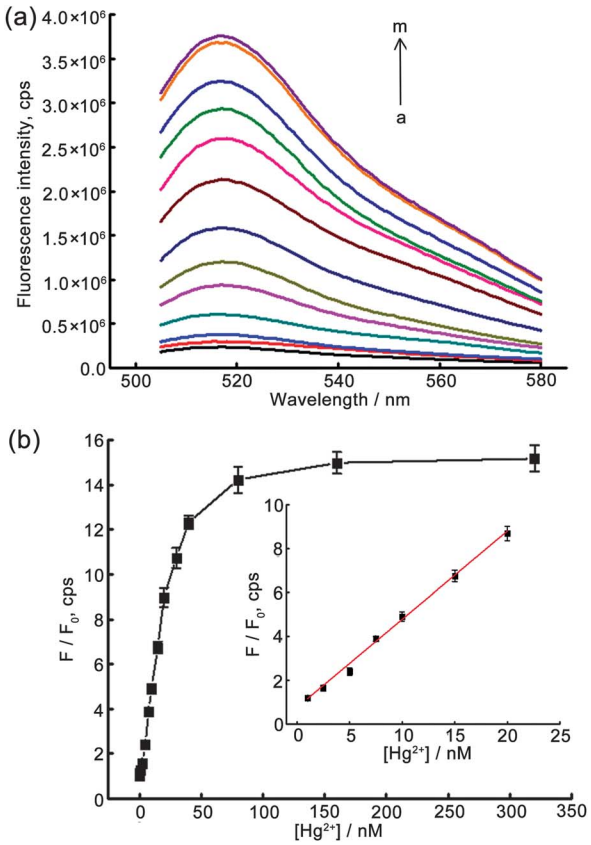

Fig. 3 (a) Fluorescence emission spectra recorded at different concentrations of target Hg^{2+}. The arrow indicates the fluorescence signal response with increasing in Hg^{2+} concentrations (0, 1, 2.5, 5, 7.5, 10, 15, 20, 30, 40, 80, 160, and 320 nM). (b) Changes of F/F_0 at 518 nm upon the addition of different concentrations of Hg^{2+}. The inset displays the linear correlation between F/F_0 and the concentrations of Hg^{2+} in the range from 1 nM to 20 nM.

Analytical performance

Under the optimal conditions, the sensitivity of the sensing system was investigated by fluorimetric titration. Fig. 3a showed the variance of fluorescence emission spectra upon the addition of different concentrations of Hg^{2+}. The fluorescence intensities of FAM enhanced significantly as the Hg^{2+} concentration was increased from 0 to 160 nM, nearly reaching a plateau after 160 nM. Fig. 3b depicts the relationship between F/F_0 and the concentrations of Hg^{2+}. The inset of Fig. 3b clearly indicated that F/F_0 was proportional to Hg^{2+} concentration in the range of 1–20 nM. The calibration equation was $F/F_0 = 0.403C + 0.696$ with a correlation coefficient of 0.9928, where C was the concentration of Hg^{2+}. The detection limit was estimated at 0.2 nM from three times the standard deviation corresponding to the background fluorescence signal. The excellent sensitivity was due to the following factors. First, the design of the split DNAzyme could not cause the stable hybridization of the DNAzyme with the MB, which ensured that the sensing system had a dramatically low background fluorescence coming from the hairpin-structured MB substrates. Second, the introduction of Hg^{2+} would induce the two separate DNAzymes to produce the activated Mg^{2+}-dependent DNAzyme. Each activated DNAzyme would hybridize with the MB substrate to form the CAMB system and catalyze the cleavage of many MB substrates through cycling and regenerating the DNAzyme, significantly amplifying each Hg^{2+}-induced DNAzyme activation event. To the best of our knowledge, this detection limit was lower than most previously reported Hg^{2+} fluorescent biosensors, and the comparisons are shown in Table 1. The maximum value of relative standard deviation (RSD) for each concentration of Hg^{2+} in the linear range was 3.9% for repeated measurements ($n = 3$), indicating the good reproducibility of our sensing strategy for Hg^{2+} detection.

Detection specificity

Besides the detection sensitivity, selectivity is another critical factor to evaluate the performance of the proposed sensing system. The specificity of the sensing strategy was investigated by comparing the fluorescence response of Hg^{2+} to that of the other metal ions such as K^+, Na^+, Ca^{2+}, Mg^{2+}, Al^{3+}, Zn^{2+}, Fe^{2+}, Fe^{3+}, Pb^{2+}, Cd^{2+}, Sn^{2+}, Co^{2+} and Cr^{3+}. These ions are the most common metal ions present in real samples. Fig. 4 depicts the fluorescence response of our sensing system for the blank solution, 20 nM Hg^{2+}, 2 μM interference metal ions, a mixture of the interference

Table 1 Comparison of fluorescence biosensors for Hg^{2+} detection

Method	Time	LOD	Ref.
FRET based on structure-switching DNA	3 min	3.2 nM	12
Self-assembly of Mg^{2+}-dependent DNAzyme	3 h	1.0 nM	41
Polymerase assisted fluorescence amplification	26 min	40 pM	24
DNA based fluorescence probe	15 min	70 nM	10
UO^{2+}-dependent DNAzyme catalytic beacons	8 min	2.4 nM	16
T_{33} probe/TOTO-3 conjugates	15 min	3.0 nM	13
Label-free DNA probe intercalation with SG	15 min	0.5 nM	32
Fluorescence enhanced by AuNPs	10 min	1.0 nM	30
T_{33} probe/TOTO-3 conjugates	15 min	10 nM	14
Fluorescence quenching by SWNTs	[a]	14.5 nM	18
Fluorescence quenching enhanced by CNPs	[a]	10 nM	17
FRET based on AuNPs and QDs	10 min	2.0 nM	27
Fluorescence labelled TBA probe	15 min	5 nM	11
FRET based on oligonucleotide probe	[a]	40 nM	7
DNA functionalized hydrogel	20 min	10 nM	15
DNAzyme cascade with CAMB	20 min	0.2 nM	This study

[a] The assay time is not mentioned in the method.

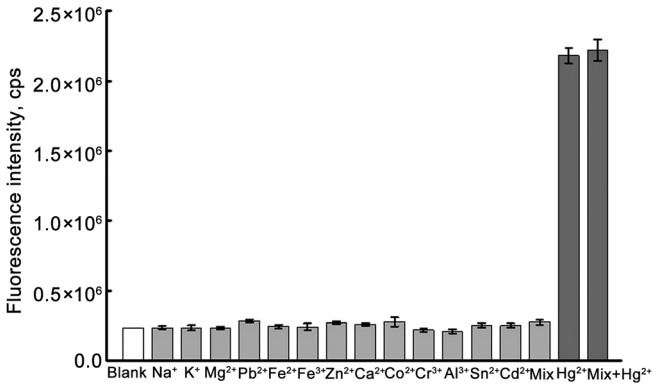

Fig. 4 Selectivity of the sensing strategy for Hg^{2+} detection over other common interference metal ions and the mixture of these metal ions. The concentration of Hg^{2+} is 20 nM, the concentrations of other metal ions are 2 μM each, and the total concentration of their mixture is 1.3 μM. Error bars show the standard deviation of three experiments.

metal ions (100 nM each) in the presence and absence of 20 nM Hg^{2+}, respectively. It could be observed that the interferential metal ions exhibited almost the same fluorescence response as the blank solution without Hg^{2+}. And the proposed sensing system could selectively detect the target Hg^{2+} even in the presence of a high-concentration mixture of the interference metal ions, which further ensured the practicality of the proposed strategy. The ultrahigh specificity was attributed to the strong coordination of Hg^{2+} to the T–T mismatched pairs.

Table 2 Recovery of Hg^{2+} in real water samples

Sample	Hg^{2+} added/nM	Hg^{2+} recovered/nM	Recovery (%)
1	0.0	0.0	—
2	2.5	$2.4^{a} \pm 0.1^{b}$	96.0
3	10.0	$10.5^{a} \pm 0.3^{b}$	105.0

[a] Mean values of four determinations. [b] Standard deviation.

Real sample analysis

In order to evaluate the practical applicability of the proposed sensing system, we further conducted Hg^{2+} detection in water samples from the Xi'an Chan River, a realistically complex sample containing a variety of interferences. The river water samples were simply filtered to remove the insoluble substances, and then spiked with target Hg^{2+} at three different final concentration levels, of 0, 2.5 and 10 nM. The recoveries of target in water samples are summarized in Table 2. The results indicate that the river water samples were free of Hg^{2+} contamination, and the proposed sensing system allows the accurate quantification of Hg^{2+} in real samples without any interference from other potentially coexisting metal ions.

Conclusions

In summary, a fluorescent sensing system was developed in this study for the highly sensitive and selective detection of Hg^{2+} in aqueous solution. This proposed strategy took advantage of the feature of the dramatically low background fluorescence of the CAMB substrate, the high specificity of T–Hg^{2+}–T coordination-induced DNAzyme activation, and the powerful signal amplification capability of the true enzymatic multiple turnovers (one DNAzyme involves in the cleavage of a number of substrates). In this way, each Hg^{2+}-induced DNAzyme activation event was successfully converted into a significantly amplified fluorescence response by cycling and regenerating the DNAzyme to realize the cleavage of many MB substrates. Eventually, a detection limit as low as 0.2 nM, much lower than those of most previously reported fluorescence assays, was achieved within a 20 min assay time in a one-step detection fashion. Moreover, this proposed sensing system showed a significantly high specificity towards target Hg^{2+}, even in the presence of a 100× excess of other interferential metal ions. The practical applications in river water samples further indicated that the sensing strategy has great potential for facile on-site and real-time Hg^{2+} sensing from a wide range of biological and environmental samples.

Acknowledgements

This research was financially supported by the National Natural Science Foundation of China (21005059), the Research Project Foundation of Shaanxi Branch of China National Tobacco Corporation, and the Fundamental Research Funds for the Central Universities.

References

1 P. M. Bolger and B. Schwetz, *N. Engl. J. Med.*, 2002, **347**, 1735–1736.
2 M. Schrope, *Nature*, 2001, **409**, 124.
3 M. Leermakers, W. Baeyens, P. Quevauviller and M. Horvat, *TrAC, Trends Anal. Chem.*, 2005, **24**, 383–393.
4 N. Pourreza and K. Ghanemi, *J. Hazard. Mater.*, 2009, **161**, 982–987.
5 B. W. Acon, J. A. McLean and A. Montaser, *Anal. Chem.*, 2000, **72**, 1885–1893.
6 N. H. Bings, A. Bogaerts and J. A. C. Broekaert, *Anal. Chem.*, 2006, **78**, 3917–3946.
7 A. Ono and H. Togashi, *Angew. Chem., Int. Ed.*, 2004, **43**, 4300–4302.
8 Y. Miyake, S. Oda, H. Yamaguchi, Y. Kondo, C. Kojima and A. Ono, *J. Am. Chem. Soc.*, 2007, **129**, 244–245.
9 Y. Miyake, H. Togashi, M. Tashiro, H. Yamaguchi, S. Oda, M. Kudo, M. Tanaka, Y. Kondo, R. Sawa, T. Fujimoto, T. Machinami and A. Ono, *J. Am. Chem. Soc.*, 2006, **128**, 2172–2173.
10 Y. W. Lin and H. T. Chang, *Analyst*, 2011, **136**, 3323–3328.
11 C. W. Liu, C. C. Huang and H. T. Chang, *Anal. Chem.*, 2009, **81**, 2383–2387.
12 Z. Wang, J. H. Lee and Y. Lu, *Chem. Commun.*, 2008, 6005–6007.
13 C. K. Chiang, C. C. Huang, C. W. Liu and H. T. Chang, *Anal. Chem.*, 2008, **80**, 3716–3721.
14 Y. W. Lin, C. W. Liu and H. T. Chang, *Talanta*, 2011, **84**, 324–329.
15 N. Dave, M. Y. Chan, P. J. J. Huang, B. D. Smith and J. Liu, *J. Am. Chem. Soc.*, 2010, **132**, 12668–12673.
16 J. Liu and Y. Lu, *Angew. Chem.*, 2007, **119**, 7731–7734.
17 H. Li, J. Zhai, J. Tian, Y. Luo and X. Sun, *Biosens. Bioelectron.*, 2011, **26**, 4656–4660.
18 L. Zhang, T. Li, B. Li, J. Li and E. Wang, *Chem. Commun.*, 2010, **46**, 1476–1478.
19 S. He, D. Li, C. Zhu, S. Song, L. Wang, Y. Long and C. Fan, *Chem. Commun.*, 2008, 4885–4887.
20 D. Liu, W. Qu, W. Chen, W. Zhang, Z. Wang and X. Jiang, *Anal. Chem.*, 2010, **82**, 9606–9610.
21 X. Liu, Y. Tang, L. Wang, J. Zhang, S. Song and C. Fan, *Adv. Mater.*, 2007, **19**, 1471–1474.
22 S. J. Liu, H. G. Nie, J. H. Jiang, G. L. Shen and R. Q. Yu, *Anal. Chem.*, 2009, **81**, 5724–5730.
23 Z. Zhu, Y. Su, J. Li, D. Li, J. Zhang, S. Song, Y. Zhao, G. Li and C. Fan, *Anal. Chem.*, 2009, **81**, 7660–7666.
24 X. Zhu, X. Zhou and D. Xing, *Biosens. Bioelectron.*, 2011, **26**, 2666–2669.
25 X. Zhou, Q. Su and D. Xing, *Anal. Chim. Acta*, 2011, **713**, 45–49.
26 D. Li, A. Wieckowska and I. Willner, *Angew. Chem., Int. Ed.*, 2008, **120**, 3991–3995.
27 M. Li, Q. Wang, X. Shi, L. A. Hornak and N. Wu, *Anal. Chem.*, 2011, **83**, 7061–7065.
28 B. C. Ye and B. C. Yin, *Angew. Chem., Int. Ed.*, 2008, **47**, 8386–8389.
29 Z. Lin, X. Li and H. B. Kraatz, *Anal. Chem.*, 2011, **83**, 6896–6901.
30 S. Cai, K. Lao, C. Lau and J. Lu, *Anal. Chem.*, 2011, **83**, 9702–9708.
31 Y. He, X. Zhang, S. Zhang, M. Baloda, A. S. Gurung, K. Zeng and G. Liu, *Biosens. Bioelectron.*, 2011, **26**, 4464–4470.
32 B. Liu, *Biosens. Bioelectron.*, 2008, **24**, 756–760.
33 D. Wu, Q. Zhang, X. Chu, H. Wang, G. Shen and R. Yu, *Biosens. Bioelectron.*, 2010, **25**, 1025–1031.
34 X. B. Zhang, R. M. Kong and Y. Lu, *Annu. Rev. Anal. Chem.*, 2011, **4**, 105–128.
35 W. Xu, Y. Xiang, H. Ihms and Y. Lu, *Rev. Fluoresc.*, 2012, **2010**, 245–268.
36 N. Dai and E. T. Kool, *Chem. Soc. Rev.*, 2011, **40**, 5756–5770.
37 C. Tuerk and L. Gold, *Science*, 1990, **249**, 505–510.
38 R. Z. Fu, T. H. Li, S. S. Lee and H. G. Park, *Anal. Chem.*, 2011, **83**, 494–500.
39 J. Achenbach, W. Chiuman, R. Cruz and Y. Li, *Curr. Pharm. Biotechnol.*, 2004, **5**, 321–336.
40 M. Hollenstein, C. Hipolito, C. Lam, D. Dietrich and D. M. Perrin, *Angew. Chem., Int. Ed.*, 2008, **47**, 4346–4350.
41 S. Shimron, J. Elbaz, A. Henning and I. Willner, *Chem. Commun.*, 2010, **46**, 3250–3252.
42 R. R. Breaker and G. F. Joyce, *Chem. Biol.*, 1995, **2**, 655–660.
43 M. N. Stojanovic, P. D. Prada and D. W. Landry, *ChemBioChem*, 2001, **2**, 411–415.
44 Y. Tian and C. Mao, *Talanta*, 2005, **67**, 532–537.
45 X. B. Zhang, Z. Wang, H. Xing, Y. Xiang and Y. Lu, *Anal. Chem.*, 2010, **82**, 5005–5011.